Supporting Information for

Ball milling assisted mechano-catalytic dye degradation using $SrTiO_3$ nanoparticles

Aman Shukla[1,2], Akshay Gaur[1], Shivam Dubey[1], Rahul Vaish[1]*

[1] *School of Mechanical & Materials Engineering, Indian Institute of Technology, Mandi, Himachal Pradesh, 175005, India.*

[2]*Department of Material Science & Engineering, Indian Institute of Technology, Kanpur, Uttar Pradesh 208016, India*

Results & Discussion

Characterisation of STO nanoparticles:

The structural characterization of STO nanoparticles was done through XRD technique. The XRD pattern, so obtained, is depicted in Figure S1, which is in complete agreement with the JCPDS card no. 35-0734 of STO[1, 2].

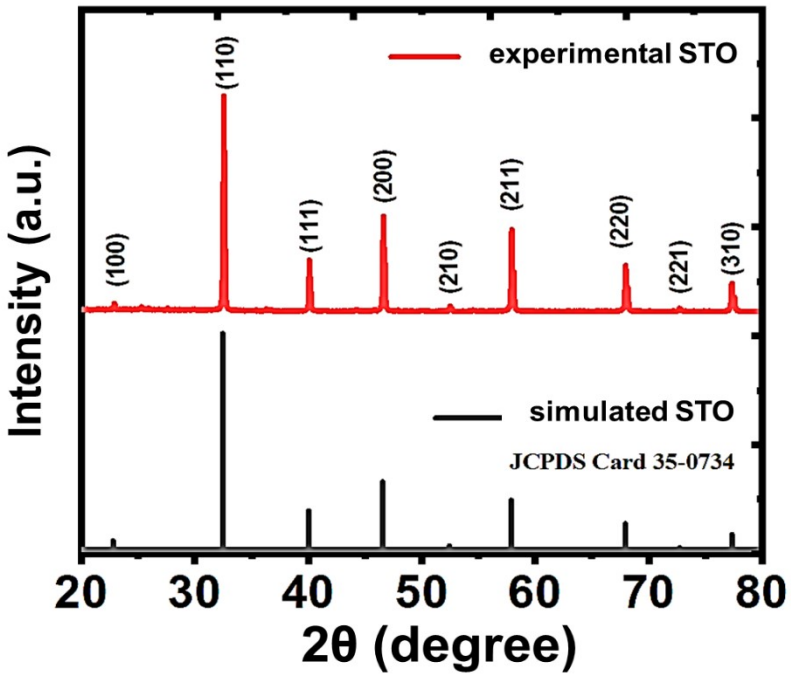

Figure S1. XRD pattern of STO nanoparticles in range of 20-80° (2θ degree).

Based on the given JCPDS card, it can be concluded that the peaks which are emerging at 22.78°, 32.45°, 40.02°, 46.55°, 52.43°, 57.88°. 67.94°, and 77.32°, are attributed to the reflections of Bragg's planes (100), (110), (111), (200), (210), (211), (220) and (310) respectively. These peaks are the signature of the cubic Pm3m perovskite phase of STO nanoparticles. STO ceramic is accommodated in the cubic unit cell, where Sr occupies the origin, Ti is positioned at the body center, and the three oxygen atoms reside at the face centers. For the (110) plane, interplanar distance d_{110} is calculated as 2.755 Å, and lattice parameter is found to be 3.899 Å, which matches perfectly with the previous reports. The average crystallite size was found to be ~48 nm, calculated using the Debye Scherer Formula.

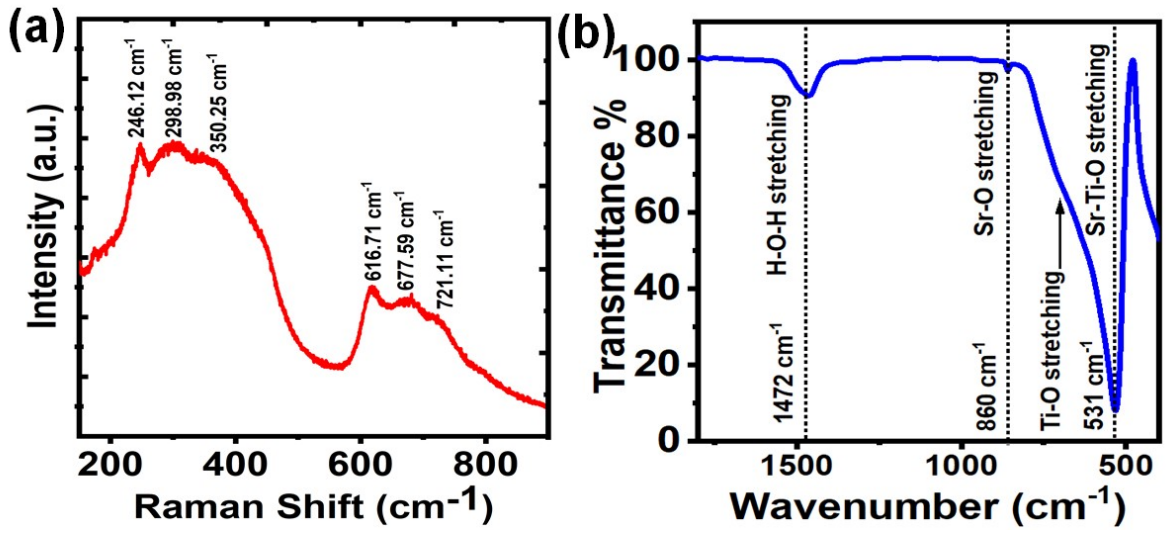

Figure S2. (a) Raman, and **(b)** FTIR spectrum of STO nanoparticles

The bonding in STO nanoparticles is confirmed by utilizing Raman Spectroscopy. Raman spectrum typically exhibits signature peaks corresponding to the optical phonon modes present in the crystal lattice. Optical phonons are vibrational modes involving the displacement of atoms within the lattice, resulting in changes in the polarization of light. In STO, the perovskite cubic crystal structure gives rise to several prominent optical phonon modes, which are often observed in the Raman spectrum as shown in Figure S2(a). Because of the cubic centro-symmetric crystal structure of STO, no first-order Raman optical phonons are observed. The two broad bands 200-400 cm^{-1} and 600-800 cm^{-1} correspond to second-order phonon modes are appeared in the spectrum.

Also, the nature of bonds present in STO was further investigated using Fourier transform infra-red spectroscopy. Figure S2(b) illustrates the FTIR spectrum of STO nanoparticles acquired within the range of 2500 cm^{-1} to 400 cm^{-1}. The presence of surface-adsorbed water molecules is indicated by the characteristic peak observed at 1472 cm^{-1}, corresponding to the H-O-H bond[3]. Additionally, a minor peak at 860 cm^{-1} signifies a weak interaction associated with the Sr-O bond within STO. The extended band spanning from 580 cm^{-1} to 700 cm^{-1} is attributed to the Ti-O stretching vibrations originating from the TiO_6 octahedron. Notably, the pronounced peak at 531 cm^{-1} signifies the stretching of the Sr-Ti-O bond[3, 4]. These discernible peaks collectively affirm the purity of the molecular composition of STO nanoparticles.

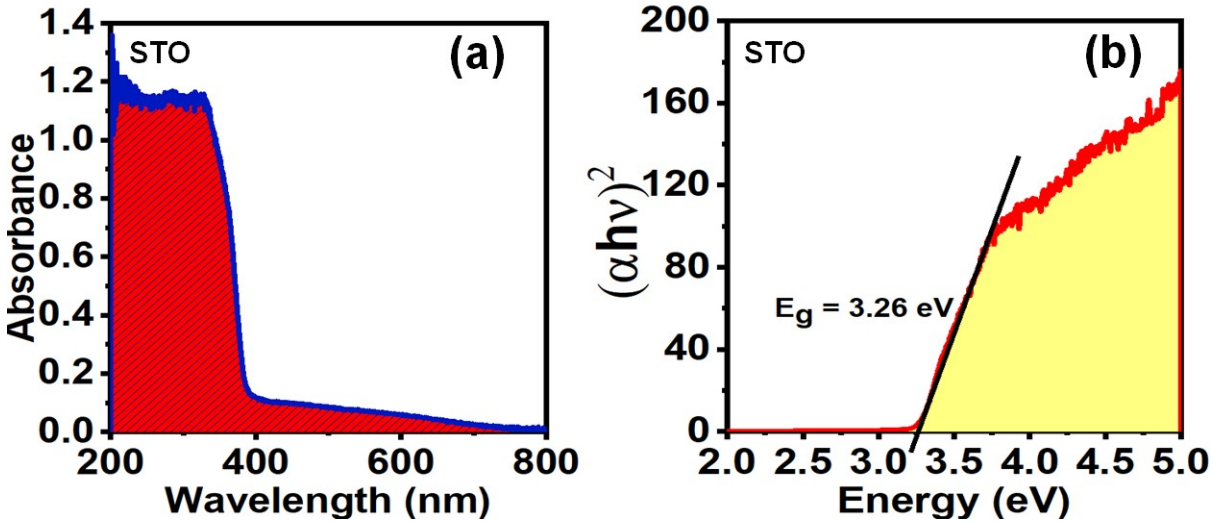

Figure S3. (a) Absorption plot showing relation between absorbance and wavelength, and **(b)** Tauc's plot revealing energy band gap of STO nanoparticles

Figure S3(a) exhibits the absorption plot of STO in the wavelength range of 200 nm to 800 nm utilizing diffused reflection spectroscopy. STO showed an absorption edge at around 386 nm. The band gap is calculated by using Tauc's equation S1:

$$(\alpha h\nu)^n = A(E_g - h\nu) \quad \text{(S1)}$$

where "α" is absorption coefficient, A is constant, "h" is Planck's constant, "ν" is frequency of incident light, "E_g" is band gap and "n" varies with nature of band gap (direct or indirect). For direct band gap materials, $n = 2$. The band gap obtained from Tauc's plot shown in Figure S3(b), is found to be 3.26 eV.

Figure S4 (a) and (b) presents the field-emission scanning electron microscopy (FESEM) images of STO nanoparticles at a scale of 2 and 5 µm. The images vividly display the spherical shape of the particles. Additionally, the inset features a particle size distribution curve in Figure S4 (a), showcasing the range of particle sizes from 100 nm to 300 nm, with an average size of approximately 182 nm. Moreover, the elemental color mapping as shown in Figure S4(c)-(e) analysis confirms the presence of Sr, Ti, and O atoms within the STO nanoparticle. This visual representation reinforces the composition of the nanoparticles.

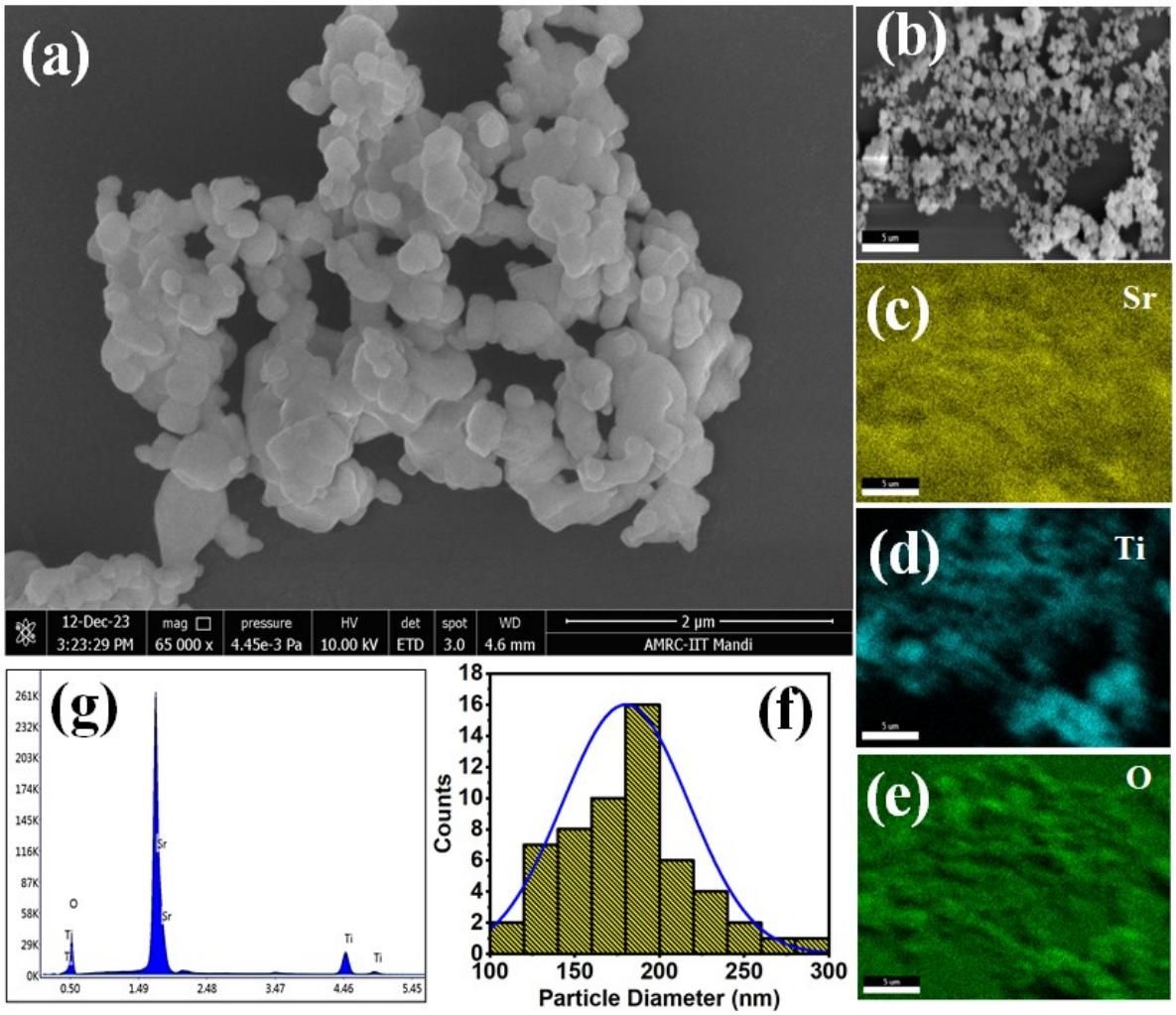

Figure S4. FESEM images of STO nanoparticles at a scale of **(a)** 2µm, **(b)** 5µm, corresponding elemental colour mapping of STO nanoparticles showing the presence of elements **(c)** Sr, **(d)** Ti, **(e)** O and (f) particle size distribution and (g) EDX spectrum of STO nanoparticles.

Furthermore, an energy-dispersive X-ray spectroscopy (EDX) spectrum was utilized to empirically quantify the weightage of constituent atoms within the molecule. The EDX spectrum reveals that the weightage of the constituent atoms closely aligns with the molecular formula, with a slightly higher amount of Sr detected. This discrepancy may be attributed to overlapping peaks of Sr and Si substrate, leading to a minor excess of Sr in the analysis.

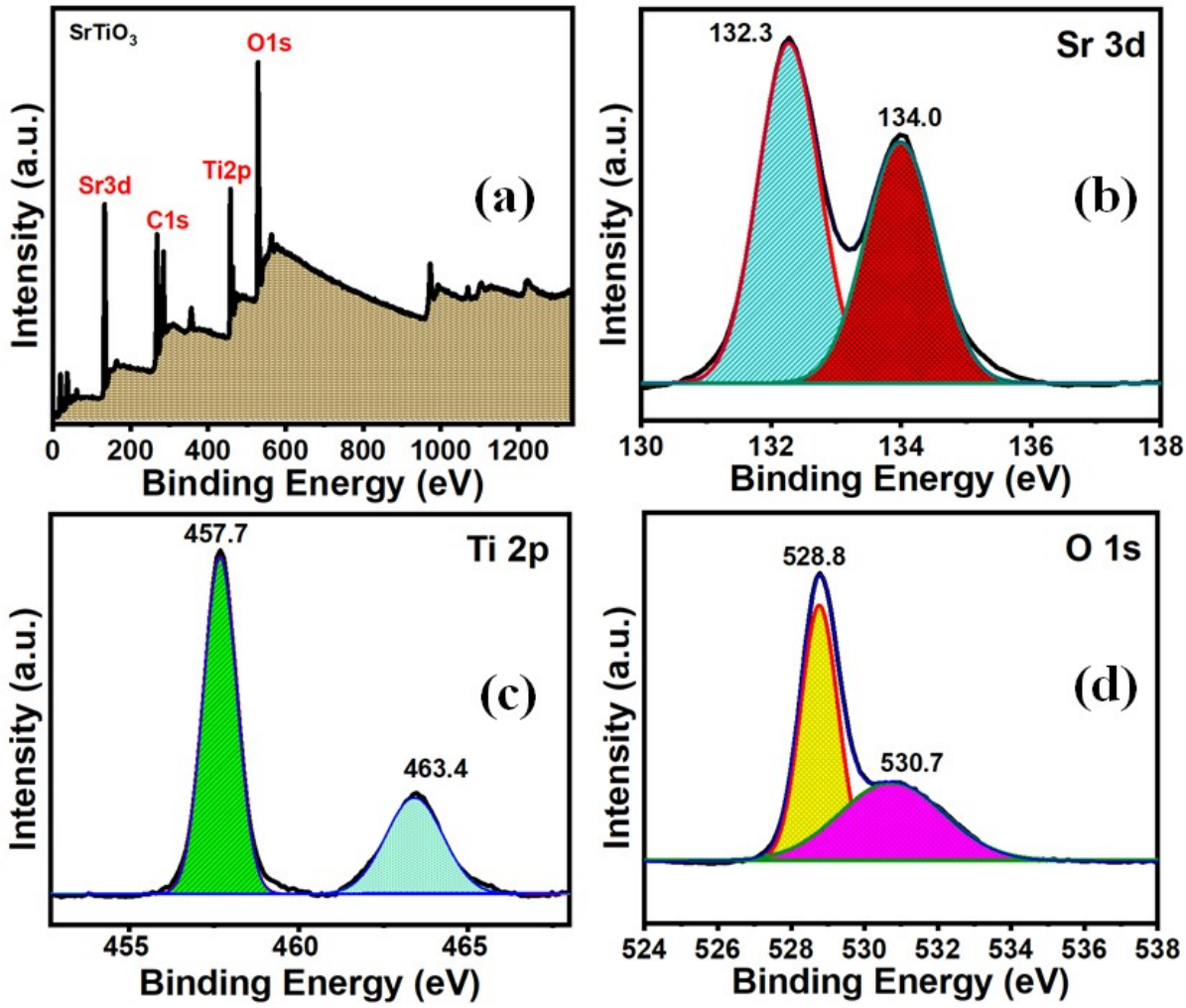

Figure S5. (a) XPS survey of STO nanoparticles in range of 0-1250 eV, deconvoluted spectrum of (b) Sr 3d, (c) Ti 2p and (d) O 1s

XPS analysis provides detailed information about the surface chemistry, oxidation states, and chemical environments of the constituent elements in STO, crucial for understanding its properties and potential applications in various fields. The core energy levels of STO, including Sr 3d, Ti 2p, and O 1s, are presented in Figure S5(a)–(d), respectively. In Figure S5(a), the overall XPS survey of STO reveals the presence of C-impurity alongside the constituent atoms Sr, Ti, and O. The deconvoluted Sr 3d spectrum as shown in Figure S5(b) exhibits a doublet of two main peaks corresponding to Sr $3d_{5/2}$ and Sr $3d_{3/2}$ components at 132.3 and 134.0 eV, respectively[5]. Figure S5(c) displays two major binding components of Ti^{4+} in the perovskite structure STO, observed as Ti $2p_{3/2}$ and Ti $2p_{1/2}$ at 457.7 and 463.4 eV, respectively[6]. Furthermore, in the O 1s spectrum, peaks centered at 530.7 eV are attributed to the O_2 state in STO, while the peak at 528.8 eV may be attributed to the presence of OH impurity or oxygen vacancies within the material[7, 8].

References:

1. Kobayashi M, Suzuki Y, Goto T, *et al.* Low-temperature hydrothermal synthesis and characterization of SrTiO3 photocatalysts for NOx degradation. *J Ceram Soc Japan*. 2018;126(2):135–138.
2. Naidu KCB, Sarmash TS, Subbarao T. Preparation and characterization of nano SrTiO3 ceramics. *Int J Phys Res*. 2014;4:1.
3. Kumar A, Sharma M, Amari A, Vaish R. Sonocatalytic induced dye degradation and antibacterial performance of SrTiO3 nanoparticles embedded cotton fabric. *Environ Res*. 2024;240:117541.
4. Xie T, Wang Y, Liu C, Xu L. New insights into sensitization mechanism of the doped Ce (IV) into strontium titanate. *Materials (Basel)*. 2018;11(4):646.
5. Chen X, Mao SS. Titanium dioxide nanomaterials: synthesis, properties, modifications, and applications. *Chem Rev*. 2007;107(7):2891–2959.
6. Shenoy US, Bantawal H, Bhat DK. Band engineering of SrTiO3: effect of synthetic technique and site occupancy of doped rhodium. *J Phys Chem C*. 2018;122(48):27567–27574.
7. Dubey S, Gaur A, Ibraheem AA, *et al.* Photo/Piezo-catalytic Performance of 0.5 Ba (Zr0. 2Ti0. 8) O3-0.5 (Ba0. 7Sr0. 3) TiO3 Ceramic. *J Mater Res Technol*. 2023.
8. Mehra S, Saroha J, Rani E, *et al.* Development of visible light-driven SrTiO3 photocatalysts for the degradation of organic pollutants for waste-water treatment: Contrasting behavior of MB & MO dyes. *Opt Mater (Amst)*. 2023;136:113344.